International Conference on Advances in Structural and Geotechnical Engineering

ICASGE'17

27-30March 2017, Hurghada, Egypt

Effect of Internal Reinforcement on the Tensile Characteristics of the UHP-SHCC Material

Amira B. Elnagar[1], Ahmed T. Baraghith[2], Hamdy M. Afefy[3]and Mohammed H. Mahmoud[4]

[1] *Master Candidate, Faculty of Engineering, Tanta University, Egypt*
E-mail:amira.elnagar.2016@gmail.com
[2] *Assistant Professor, Faculty of Engineering, Tanta University, Egypt*
E-mail:ahmed.baraghit@f-eng.tanta.edu.eg
[3] *Associate Professor, Faculty of Engineering, Tanta University, Egypt*
E-mail:hamdy.afefy@f-eng.tanta.edu.eg
[4]*Professor, Faculty of Engineering, Tanta University, Egypt*
E-mail:mohammed. hussein@f-eng.tanta.edu.eg

ABSTRACT

Ultra-High-Performance Strain-Hardening Cementitious Composites (UHP-SHCC) is one form of fiber reinforced composites, which has high compressive and tensile strengths along with high strain capacity in tension with strain hardening plateau. Obviously, proper selection of strengthening/retrofitting material plays an important role in restoring the lost capacity of the strengthened/retrofitted member. This paper investigated experimentally the effect of internal reinforcement in the UHP-SHCC specimens on the tensile strength as well as the cracking characteristics. Seven UHP-SHCC specimens with identical dimensions of 500 x 150 x 50 mm were tested under pure axial tension. Different configurations of the internal reinforcement were considered; namely, internal orthogonal mesh of clear spacing of 50 mm in both directions, or smooth bars of 6 mm diameter. For both configurations, different reinforcement ratios were considered. The experiential results showed that the internal mesh configuration enabled the specimen to develop better crack distribution along with higher tensile capacity compared to those of specimens having internal smooth bars configurations. In addition, increasing the internal reinforcement ratio resulted in increase the tensile strength of the UHP-SHCC as well as reduce the average crack spacing.

Keywords: Reinforced Concrete, Axial Tension, UHP-SHCC, Strengthening, Material.

INTRODUCTION

Recently, Ultra-High-Performance Strain-Hardening Cementitious Composites (UHP-SHCC) have been used for strengthening/retrofitting of different structural applications. This material is a new generation of fiber reinforced cementitious composites, which has high tensile ductility and durability characteristics along with strain-hardening plateau [1-4]. Because of the improved characteristics of the UHP-SHCC material in both compression and tension, it exhibited remarkable results in increasing and/or restoring the ultimate load carrying-capacity of reinforced concrete members when provided in either compression or tension side in the members [5-9].

The effect of small amount of reinforcement ratio on the UHP-SHCC tension members has been investigated in order to enhance the post cracking behavior [5]. The ability of the proposed steel reinforcement to preclude the localized fracture and consequently to improve the post-cracking behavior of UHP-SHCC under axial tension have been studied [10-11]. It has been found that by increasing the reinforcement ratio, the averaged cracks spacing had gradually decreased. In addition, uniaxial tensile tests, zero-span tensile tests and flexural tests have been conducted in order to study the efficiency of the SHCC as a repair material [3]. It was concluded that in both zero-span tensile tests and flexural tests, the width of cracked regions of RC repaired specimens was quite limited compared to that of the uniaxial tensile tests. Furthermore, It was found that increasing the reinforcement ratio changed the mode of

failure of the SHCC-strengthened beams from brittle to more ductile one [13]. Also, it has showed that the combination of SHCC and a small amount of steel reinforcement helped in the development of higher strain in the SHCC strengthening layer at the ultimate load and eliminated early strain localization. In addition, recovery of protective performance of cracked Ultra High-Performance Strain-Hardening Cementitious Composites (UHP-SHCC) due to autogenous healing have been investigated by Kunieda et al. [14].

The flexural performance of reinforced concrete beams with a polyethylene (PE) fiber reinforced with strain-hardening cement-based composite (SHCC) layer in tension zone have been investigated by Yang et al. [15]. It was found that the flexural strength, distribution of cracks, and flexural properties of the expansive SHCC-layered reinforced concrete beams are better than that of the conventional reinforced concrete beams. Furthermore, it was found that UHP-SHCC strengthening material increased the load carrying capacity [16]. Moreover, the influence of the Brazilian raw materials on the mechanical performance of Strain Hardening Cementitious Composites (SHCC) have been studied by Magalhães et al. [17]. Zhang [18] investigated a zero-span tensile model with fictitious material. It has been proven that the cracking behavior of SHCC used for flexural strengthening of RC members is affected by the SHCC thickness.

In the current research, the effect of providing either longitudinal smooth steel bars of 6 mm diameter or orthogonal meshes of 3 mm bars diameters on the tensile characteristics of the UHP-SHCC material has been investigated.

EXPERIMENTAL PROGRAM

Test specimens

Seven UHP-SHCC specimens with typical cross-sectional dimensions of 50 mm by150 mm and specimen length of 500 mm were tested under direct tension test. Different reinforcement ratios (ranging from 0.3 to 1.1%) and reinforcement configurations (bars or meshes) have been studied. Smooth bars of 6mm diameter (D6) and orthogonal steel mesh (#) formed from smooth bars of 3 mm diameter were used as internal reinforcement as summarizes in Table 1. Three deformed bars of 16 mm diameter (D16) were provided at both ends of the specimens in order smoothly transfer the direct tensile force to the UHP-SHCC specimens as depicted in Fig. 1. As Illustrated in Table 1, specimens S-1D6, S-2D6 and S-3D6 were reinforced with one, two and three smooth bars of 6 mm diameter, respectively, while specimens S-1#, S–2# and S–3# were reinforced with one, two and three orthogonal mesh of 3 mm bar diameter, respectively.

Table 1: Description of test specimens

Specimen	Dimensions (mm)	Internal reinforcement	Internal reinforcement ratio, %
S – 0	500x150x50	-----	0
S – 1D6	500x150x50	1D6	0.4
S – 2D6	500x150x50	2D6	0.8
S – 3D6	500x150x50	3D6	1.1
S – 1#	500x150x50	1#	0.3
S – 2#	500x150x50	2#	0.6
S – 3#	500x150x50	3#	0.9

Material properties

Table 2 summarizes the mix proportions of the used UHP-SHCC material. The water to binder ratio (W/B) was 0.20. Low heat Portland cement of density = 3.14 g/cm^3 was used, while 15% of the design cement content was substituted with a silica fume (density= 2.2 g/cm^3). Quartz sand (density= 2.68 g/cm^3) was used as the fine aggregate. High strength polypropylene (PP) fiber was chosen with fiber volumetric ratio of 1.5%. The diameter and length of the PP fibers were 0.012 mm and 6 mm, respectively. In addition, superplasticizer was used in order to enhance the workability of the matrix. After demolding, all the specimens were treated by water for 28 days till the testing day. For the UHP-SHCC material, compression tests were performed on six standard cubes of 150 mm side length in order to obtain the UHP-SHCC compression strength. The averaged indirect tensile strength based on split

cylinder test, compressive strength and tensile strain of the UHP-SHCC at the age of 28 days were determined to be 4.6 MPa, 65 MPa and 1.2%, respectively. The average yield strength, tensile strength and Young's modulus for the used D6 bars were 270 MPa, 529 MPa and 215 GPa respectively. While, the average yield strength for the orthogonal mesh of 3 mm bars diameters was 320 MPa.

(a) Specimen provided by 1D6 bar (S-1D6) (b) Specimen provided by three orthogonal mesh (S-3#)

Fig. 1: The internal reinforcement illustration longitudinal bar and mesh configurations.

Table 2: Mix proportions of UHP-SHCC.

Water/ Binder ratio	Unit content (kg/m^3)							
	Water	Cement	Silica fume	Expansion agent	Sand	Super plasticizer	Air reducer	PP Fiber (6mm)
0.20	292	1243	223	20	149	14.9	2.98	14.6

Test setup and procedures

The tensile force was applied on the tested specimens by gripping the steel bars at the specimen's ends as shown in Fig.1. The test was carried out using a universal testing machine operated in load controlled mode. Four Pi-shaped displacement transducers with a gauge length and accuracy of 100 mm and 0.005 mm, respectively, have been used to record the developed deformations during the test (refer to Fig. 2). Thus, the average deformation along with the average tensile strain could be obtained.

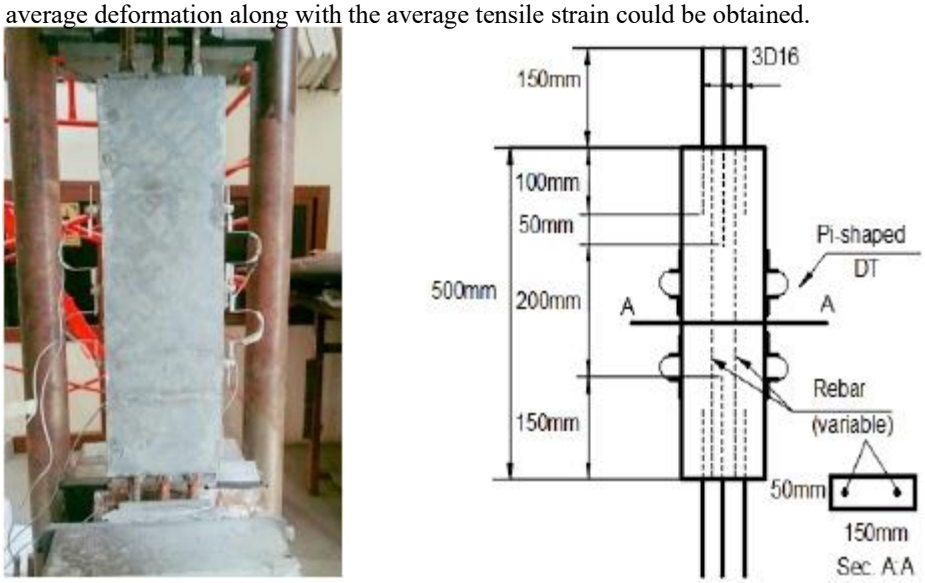

Fig. 2: Test setup and instrumentation.

TEST RESULTS AND DISCUSSION

Table 3 summarizes the experimental results for all specimens considering the first cracking load, ultimate load, number of cracks and the maximum, minimum and average crack spacing.

Table 3: Experimental results

Specimen	Load		Cracks			
	P_{cr} (kN)	P_u (kN)	S_{cr-av} (mm)	S_{cr-max} (mm)	S_{cr-min} (mm)	N
S – 0	20.3	25.8	45.2	105	10	5
S – 1D6	19.1	36.5	15.6	37	5	15
S – 2D6	18.6	41	12	18	5	18
S – 3D6	18.1	48	8.3	15	3	31
S – 1#	18.2	42	20.4	50	5	12
S – 2#	20.3	51	12	35	5	22
S – 3#	21.1	55	12	20	4	25

P_{cr} = first cracking load, P_u = ultimate load, S_{cr-av} = average crack spacing, S_{cr-max}= maximum crack spacing, S_{cr-min} = minimum crack spacing, N=number of cracks,

Effect of the internal reinforcement on the tensile strength

Fig. 3 shows the tensile stress-strain curves of the control un-reinforced specimen as well as the reinforced specimens with both 6 mm bars (S-1D6, S-2D6 and S-3D6) and orthogonal mesh (S-1#, S–2# and S–3#). For all specimens, the stress-strain relationship was linear and approaching zero till the appearance of the first crack, and then the strain increased significantly. With further loading cracks were spread along the middle part of the specimens. After the first tensile crack, strain hardening accompanied by multiple cracking distributed over the tensile specimens was exhibited till the ultimate load for all specimens. As shown in Figs. 3(a and b), the control specimen showed limited tensile strain after reaching the maximum tensile strength, however, the provided internal reinforcement enabled the UHP-SHCC specimen to exhibit some ductile tensile plateau. Although, the specimens provided by internal orthogonal meshes showed higher tensile plateaus accompanying by higher tensile strengths. Increasing the reinforcement ratio for both configurations resulted in increased ultimate capacity proportionally. The strain response of the six reinforced specimens indicated 3 stages up to failure. Stage 1, before first crack which is similar to the control specimen behavior. Stage 2, there has been a significant effect of steel reinforcement and fiber orientation of the UHP-SHCC up to the maximum tensile strength. Stage 3, the softening stage, while the internal reinforcement was yielding and the tensile strength of the UHP-SHCC material was exhausted.

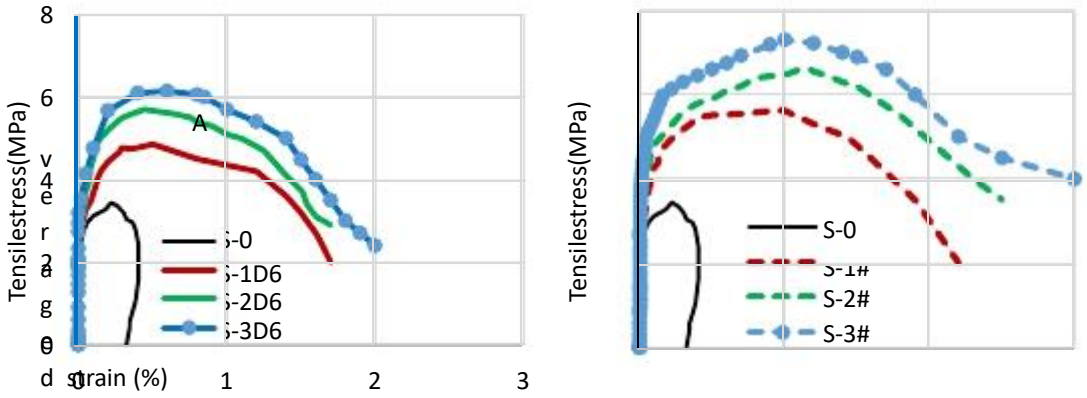

(a) Specimens provided by 6 mm bars diameters

(b) Specimens provided by orthogonal mesh of 3 mm bars diameters

Fig. 3: Tensile stress-strain curve for all specimens.

Effect of internal reinforcement on cracking and ultimate load

As summarizes in Table 3, the cracking and ultimate loads of the tested two configurations as well as the control specimens are presented. Based on the test results it was observed that the internal reinforcement has slight adverse effect on the first cracking load. That could attributed to the higher shrinkage strain

developed by the UHP-SHCC owing to the high cement content which restrained by the internal reinforcement. Thus, the reinforced UHP-SHCC may show hair cracks at a load level lower than that of the UHP-SHCC specimen without internal reinforcement. On the other hand, internal reinforcement showed significant effect on the maximum tensile load. Fig. 4 shows the variations of both cracking and ultimate loads with the reinforcement ratio for both reinforcement configurations. It could be observed that increasing the reinforcement ratio resulted in increase the ultimate load gradually. That is because the ultimate load of reinforced specimens is equal to the sum of the contributions from the internal fibers and provided internal steel reinforcement. Thus, the use of internal reinforcement results in decreasing the internal fibers stress, just after cracking, and consequently enables the specimen to attain higher ultimate load compared to that of the unreinforced specimen.

For the first configuration, (S-3D6) that has reinforcement ratio of 1.1% exhibited the highest ultimate capacity, while specimen S-3#, which has reinforcement ratio of 0.9 exhibited the highest ultimate tensile capacity among all specimens of both configurations. That means providing orthogonal mesh showed higher effect on the tensile capacity compared to that resulted from providing longitudinal bars even though the reinforcement ratio was lower than that of the longitudinal bars.

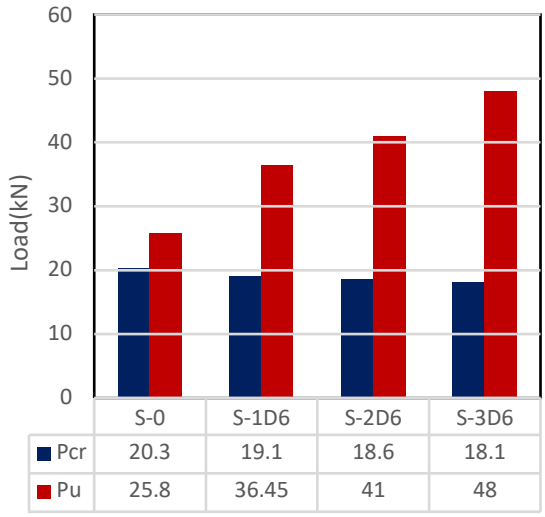

(a) Specimens provided by bars of 6 mm diameters

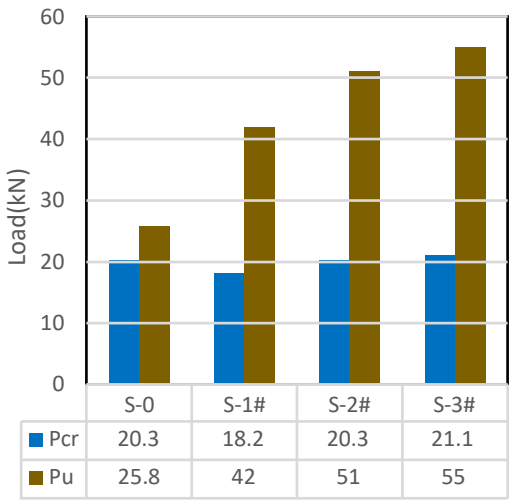

(b) Specimens provided by orthogonal mesh of 3 mm bars diameters

Fig. 4: Ultimate tensile load and cracking load versus reinforcement ratio of the internal reinforcement for all specimens.

Effect of internal reinforcement on tensile load

Figure 5 shows the relationship between the load of all tested specimens and the averaged strain. For all specimens, the load-average strain relationship is linear up to the first cracking load with a very stiff response. After cracking, the stiffness reduced significantly. It can be noticed that the response of unreinforced specimen S-0 is brittle failure associated with a very limited strain hardening response. The load-average strain response of the reinforced specimens by either longitudinal bars or orthogonal mesh is approximately equal to the contribution of both the UHP-SHCC material and the internal steel reinforcement.

For the reinforced specimens, the response of the load-average strain relationship can be divided into three regions. In the first region, the behavior is similar to that of the unreinforced specimen, since the contribution from the internal steel reinforcement is minor. In the second region, the micro-cracking increase and then a transition zone is entered when the internal steel reinforcement is fully activated to counteract the stiffness degradation of the UHP-SHCC. Thus, the response in this region is due to the contribution from the internal fibers of the UHP-SHCC material and the internal steel reinforcement and

consequently it is mainly dependent on their properties. Finally, in the third region, the strain in the internal steel reinforcement exceeds its yield strain and its contribution becomes almost constant, whereas the contribution from the fibers continues to increase up to failure of the specimen which corresponds to the occurrence of the reinforcing fibers debonding. It can be observed that the orthogonal mesh enabled the internal fibers to work properly compared to the longitudinal bars, since the specimens provided by orthogonal mesh exhibited more ductile response while the contribution of both longitudinal bars and the orthogonal mesh was approximately the same as depicted in Fig. 5.

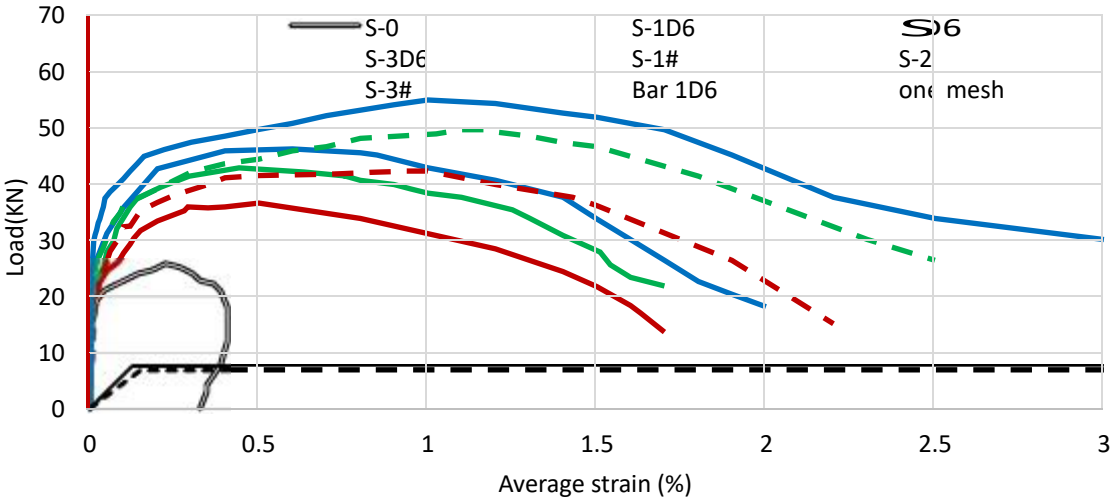

Fig. 5: Load-Averaged strain restraint for all tested specimens.

Effect of internal reinforcement on cracks distribution and number

Figure 6 shows cracks mapping after complete tensile failure for both configurations. It could be observed that the cracks distributions are almost the same for both configurations while cracks localizations are developed for the case of longitudinal bars as depicted in Fig. 6(a). Moreover, all the reinforced specimens developed more cracks compared with unreinforced specimens. Obviously, the enhancements of cracking behavior in the reinforced UHP-SHCC specimens may be attributed to the increase in the axial stiffness at cracks due to the contribution from the internal steel reinforcement, which enables the formation of more transverse cracks and carrying of higher loads.

In order to quantify the average crack spacing for both configurations, the developed total number of cracks are compared against the internal reinforcement ratio for both configurations as depicted in Fig. 6. For both configurations, it can be noticed that increasing the reinforcement ratio of the internal reinforcement enabled the reinforced UHP-SHCC specimen to develop more cracks. However, at the same reinforcement ratio the orthogonal mesh configuration enabled the specimen to show more crack, especially when the reinforcement ratio was in between 0.4% to 0.9% as depicted in Fig. 7.

Considering the average crack spacing, both configurations show approximately the same value at the same reinforcement ratio as depicted in Fig. 8.

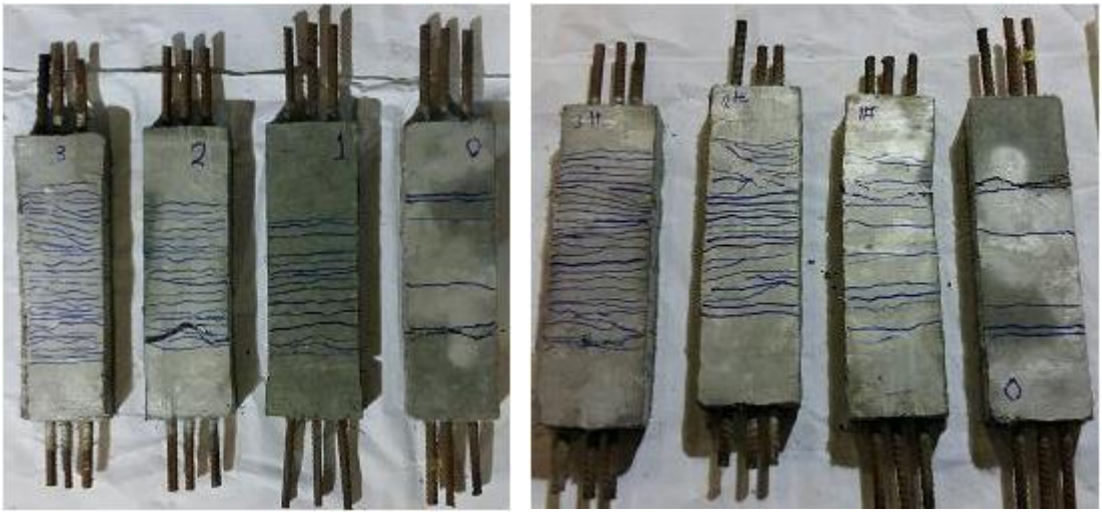

(a) Specimens provided by bars of 6 mm diameters

(b) Specimens provided by orthogonal mesh of 3 mm bars diameters

Fig. 6: Cracks distribution for all specimens.

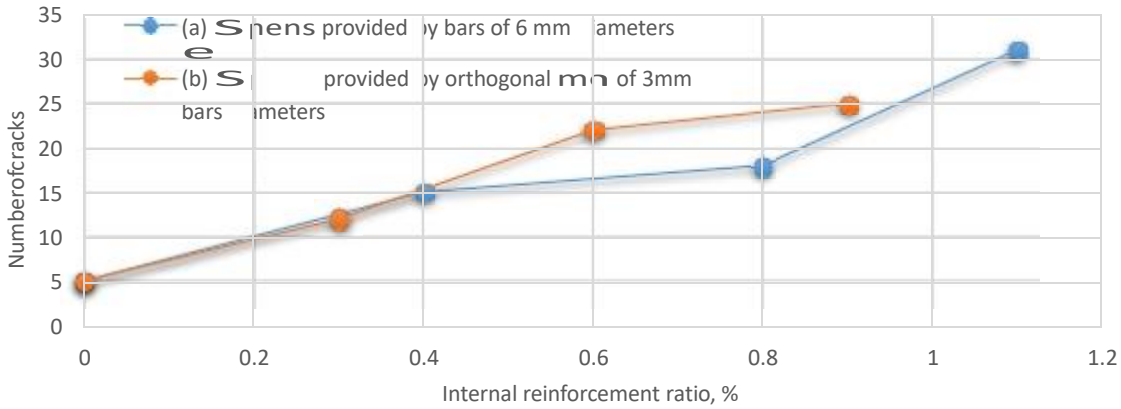

Fig. 7: Number of cracks versus reinforcement ratio of the internal reinforcement for all specimens.

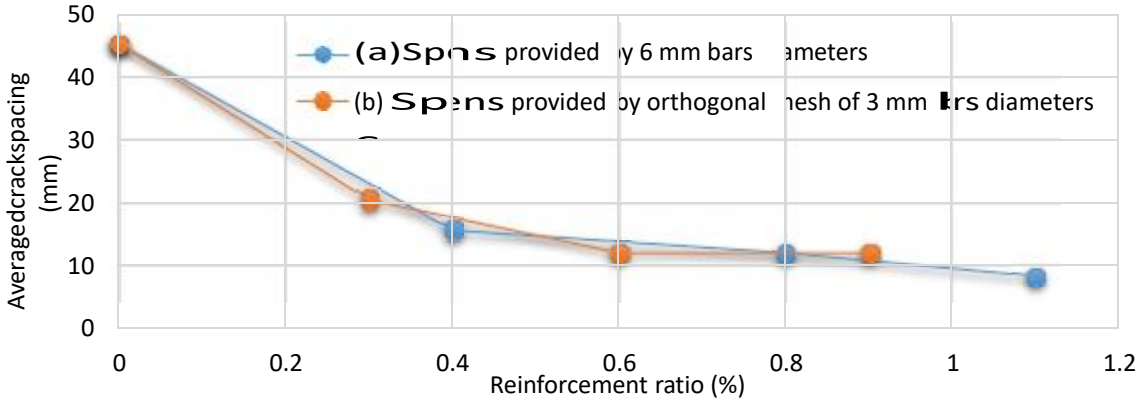

Fig. 8: Average cracks spacing for all specimens versus reinforcement ratio.

CONCLUSION

The current paper investigated experimentally the effect of internal reinforcement in the UHP-SHCC specimens on the direct tensile strength as well as the cracks propagations. Based on the studied reinforcement configurations along with reinforcement ratios, the following conclusions could be drawn: -

1- Providing internal reinforcement in the UHP-SHCC material affects slightly the first cracking load, while it affects the ultimate tensile capacity significantly.
2- Increasing the reinforcement ratio results in increase the tensile capacity of the UHP-SHCC material. That is for both internal longitudinal bars and orthogonal mesh.
3- The orthogonal mesh configuration helped the UHP-SHCC to exhibit enhanced cracks distribution along with enhance tensile capacity compared to specimens provided by longitudinal bars having the same reinforcement ratio. Thus, specimen S-3# showed the most enhanced performance among all test specimens.

REFERENCES

[1] Li, V. C., (1993), "From micromechanics to structural engineering: the design of cementitious composites for civil engineering applications" JSCE Journal of Structural Mechanics and Earthquake Engineering, Vol. 10, pp. 37-48.
[2] Kunieda, M., Denarie, E., Bruhwiler, E., Nakamura, H., (2007), "Challenges for strain hardening cementitious composites-deformability versus matrix density" Proc. of the 5th Int. RILEM workshop on HPFRCC, pp. 31-38.
[3] Kamal, A., Kunieda, M., Ueda, N., Nakamura, H., (2008), "Evaluation of crack opening performance of a repair material with strain hardening behavior" Cement and Concrete Composites, Vol. 30, No. 10, pp. 863–871.
[4] Kunieda M, Ueda N, Nakamura H, Tamakoshi T., (2009), "Development of spraying technique for UHP-SHCC" Proc. of the Concrete Structure Scenarios Vol. 9, pp. 349–354.
[5] Kunieda M, Hussein M, Ueda N, Nakamura H., (2010), "Enhancement of crack distribution of UHP-SHCC under axial tension using steel reinforcement" J Adv Concr Tech Vol. 8, pp. 49-57.
[6] Afefy H. M., Fawzy T. M., (2013), "Strengthening of RC one-way slabs including cut-out using different techniques" Engineering Structures Vol. 57C, pp. 23-36.
[7] Afefy H. M., Mahmoud M. H.,(2014), "Structural performance of RC slabs provided by pre-cast ECC strips in tension cover zone" Construction and Building Materials Vol. 65, pp. 103-113.
[8] Afefy H. M., Kassem N., Hussein M., (2015), "Enhancement of flexural behavior of CFRP-strengthened reinforced concrete beams using engineered cementitious composites transition layer" Structure Infrastructure Engineering Vol. 11, pp. 1042-1053.
[9] Afefy H. M., Kassem N. M., Mahmoud M. H., Taher S. F., (2016), "Efficient strengthening of opened-joint for reinforced concrete broken slabs" Composite Structures Vol. 136, pp. 602-615.
[10] M. Kunieda, M. Hussein, N. Ueda and H. Nakamura. (2010), "Fracture behavior of steel reinforced UHP-SHCC under axial tension", Korea Concrete Institute, pp.1557-1564.
[11] M. Kunieda, K. Kozawa, N. Ueda and H. Nakamura. (2010), "Fracture analysis of strain hardening cementitious composites by means of discrete modeling of short fibers", Proceedings of FraMCoS, Vol.28, pp. 501–508.
[12] Minoru Kunieda, Hiroki Ogura, Naoshi Ueda,and Hikaru Nakamura. (2011), "Tensile fracture process of Strain Hardening Cementitious Composites by means of three-dimensional meso-scale analysis", Cement & Concrete Composites, Vol. 33, pp. 956–965.
[13] Mohamed Hussein, Minoru Kunieda, Hikaru Nakamura,(2012), "Strength and ductility of RC beams strengthened with steel-reinforced strainhardening cementitious composites", Cement & Concrete Composites, Vol.34, pp. 1061–1066.
[14] Minoru Kunieda, Kang Choonghyun, Naoshi Ueda, andHikaru Nakamura,(2012), "Recovery of protective performance of cracked Ultra High Performance Strain Hardening Cementitious Composites (UHP-SHCC) Due to Autogenous Healing", Journal of Advanced Concrete Technology, Vol. 10, pp. 313–322.
[15] Hae Jun Yang, June Su Kim, Sung Ho Kim, and Hyun Do Yun.(2012), "Flexural Performance of Reinforced Concrete Beams with a Layer of Expansive Strain-hardening Cement –based Composite(SHCC)", Chungnam National University, Korea (WCEE 15),pp.1–5.

[16] Ahmed Kamal, Minoru Kunieda, Naoshi Ueda, and Hikaru Nakamura, (2008), "Assessment of strengthening effect on RC beams with UHP-SHCC", JCI annual meeting , Vol.30, pp. 1483-1488.
[17] Margareth da Silva Magalhãesa, Romildo Dias Toledo Filhob, and Eduardo de MoraesRegoFairbairnb, (2014), " Influence of Local Raw Materials on The Mechanical Behavior and Fracture Process of PVA-SHCC", Materials Research, Vol.17, pp 146-156.
[18] Yongxing Zhang, (2013) , "Zero-span tensile model for evaluating cracking behavior of SHCC for RC flexural strengthening", Magazine of Concrete Research, Vol. 65, pp.1486–1493.